Title	Fault tolerant control of harmonic injected nine-phase flux switching permanent magnet motor drive system
Author(s)	Yu, F; Cheng, M; Li, F; Chau, KT; Huang, J; Hua, W
Citation	The 17th International Conference on Electrical Machines and Systems (ICEMS 2014), Hangzhou, China, 22-25 October 2014. In Conference Proceedings, 2014, p. 3117-3122
Issued Date	2014
URL	http://hdl.handle.net/10722/217353
Rights	International Conference on Electrical Machines and Systems (ICEMS). Copyright © IEEE.

Fault Tolerant Control of Harmonic Injected Nine-Phase Flux Switching Permanent Magnet Motor Drive System

Feng Yu[1], Ming Cheng[1*], Feng Li[1], K. T. Chau[2], Jin Huang[3], Wei Hua[1]
[1] School of Electrical Engineering, Southeast University, Nanjing 210096, China
[2] Department of Electrical and Electronic Engineering, The University of Hong Kong, Hong Kong
[3] College of Electrical Engineering, Zhejiang University, Hangzhou 310027, China.
E-mail: mcheng@seu.edu.cn

Abstract—In this paper, a universal online generation technique of non-sinusoidal fault-tolerant current is proposed for a nine-phase flux switching permanent magnet (NP-FSPM) motor with third harmonic back electromotive force (EMF) under single phase open-circuit fault condition. The decoupled model of NP-FSPM motor has been developed. By calculating the average torque and the pulsating torque components in steady state, the condition for reducing the torque ripple is analyzed, and the third harmonic current injection can be kept constant in the pre- and post open-circuit fault condition. The predicted results are confirmed by simulation.

I. INTRODUCTION

Stator permanent magnet (PM) machines including doubly salient permanent magnet (DSPM) machine, flux reversal permanent magnet (FRPM) machine and flux switching permanent magnet (FSPM) machine, have attracted wide attention due to their simple and robust structure, easy thermal management. It has been identified that the FSPM machine can offer higher power density, and fault-tolerance capacities, as compared with other type of stator PM machine [1]. Hence, three phase FSPM motors have been widely researched for application in aerospace, navigation and electric/hybrid vehicles (EV/HEV) recently [2-3].

Except three phase motors, multiphase flux-switching permanent-magnet (FSPM) motor drives are emerging as a key enabling technology for safety critical application, such as electric vehicles, ultrahigh speed elevators [4-6]. Due to the additional degree of freedom, it is convenient to derive the disturbance-free operation condition of this multiphase FSPM motor in terms of some fault-tolerant control methods, whereas the fault-tolerant control in a three-phase machine requires additional hardware or electrically isolated phases [7-9].

Open-circuit fault-tolerant operation of multiphase (below six) motors with sinusoidal back electromotive force (EMF) and sinusoidal phase currents are reported in [10-12]. Generally, it is assumed that such fault-tolerant machines have a sinusoidal back EMF waveform, so that the current controller is required to track a set of sinusoidal current commands proportional to a given torque demand. Solutions for fault-tolerant currents are obtained from the condition to produce undisturbed rotating magneto-motive force (MMF) by using the traditional phasor representation of the stator currents in the healthy phases [10]. Such control methods are not applicable to the nine-phase FSPM (NP-FSPM) motor in this paper, since they may inevitably result in an undesirable low-frequency torque pulsation under a fault condition because of the non-sinusoidal flux linkage due to flux path variation with rotor position and full-pitch concentrated windings design.

The purpose of this paper is to propose a new fault-tolerant control for multiphase FSPM motor with non-sinusoidal back-EMF. In Section II, third harmonic current injection method is presented. In Section III, a universal online generation technique of non-sinusoidal fault-tolerant current and optimization objectives of the NP-FSPM motor drive are analyzed numerically. To predict normal and fault responses, a transient Matlab/Simulink model for fault analysis is developed and simulation is carried out in Section IV. Finally, conclusions are drawn in Section V.

II. ANALYSIS AND DERIVATION

A. FSPM Motor Modeling

A full-pitch concentrated windings FSPM machine with 34-rotor-pole and 36 stator-tooth has been proposed, featuring only odd-order harmonics in the air-gap MMF distribution, as shown in Fig. 1. The stator consists of "U-shaped" laminated segments, between which circumferentially magnetized magnets are sandwiched and the direction of magnetization is reversed from one magnet to the next. Each stator tooth comprises two adjacent laminated segments and one magnet. There are four coils in each phase, and each coil surrounding only one tooth. The resultant MMF waveform will be established by nine, equally spaced phase windings. Due to the fact that there are no magnets, brushes, nor windings in the rotor, the NP-FSPM machine offers the advantages of simple structure and mechanical robustness [1].

Finite-element method (FEM) is used to calculate the back-EMF of the NP-FSPM motor. Fig. 2(a) shows the first three no-load back EMF waveform of the motor. The amplitude of the back EMF is 288V, and the waveform is

This work was supported by the National Key Basic Research Program (973 Program) of China under Project 2013CB035603).

distorted. The fast Fourier transform (FFT) is carried out to obtain its frequency components in Fig. 2(b). It is found that the most significant harmonic in the back-EMF waveform is the third-order harmonic while higher order harmonics are relatively low. Neglecting the influence of the higher order harmonics, phase voltages can be obtained as:

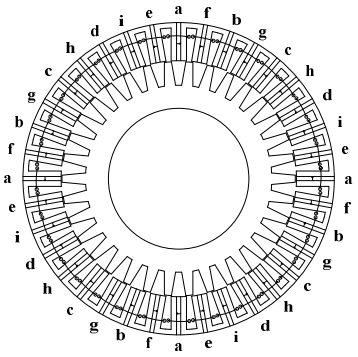

.Fig. 1 Cross section of the nine-phase FSPM motor.

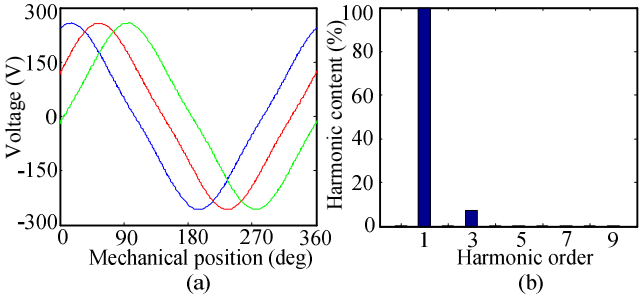

Fig. 2 Back EMF. (a) Waveform. (b) FFT results.

$$\begin{cases} e_a = E_1 \sin(\omega t) + E_3 \sin(3\omega t + \varphi_3) \\ e_b = E_1 \sin(\omega t - \dfrac{2\pi}{9}) + E_3 \sin(3\omega t - \dfrac{6\pi}{9} + \varphi_3) \\ \vdots \\ e_i = E_1 \sin(\omega t - \dfrac{16\pi}{9}) + E_3 \sin(3\omega t - \dfrac{48\pi}{9} + \varphi_3) \end{cases} \quad (1)$$

where ω is the frequency of the fundamental component (the electrical rotor speed), φ_3 is the 3-order harmonic angle relative to the fundamental component, E_1 and E_3 are the amplitudes of the fundamental and 3-order harmonic back EMF, respectively.

B. Third Harmonic Current Injection

By using symmetrical linear transformations [13], it is possible to represent the nine phase currents by four independent space vectors in different α-β planes. Hence, the spatial distribution of the MMF produced by the stator windings in the air gap can be written as a function of these space vectors in the following compact form:

$$F_s(\theta_s, t) = \frac{9N_s}{2\pi p} \sum_{h=1,3,\ldots}^{7} K_{wsh} \Re_e\left(\bar{i}_h(t) e^{jh\theta_s}\right) \quad (2)$$

where N_s is the number of conductors in series per phase, K_{wsh} is the hth winding coefficient, p is the number of pairs of poles, θ_s is a stationary angular coordinate, $\bar{i}_h$ is the hth stator current space vector, and $\Re_e$ is real part.

The MMF relationship in (2) takes into account the first (M-2) spatial harmonics, and is valid both in steady-state and transient conditions. In particular, its amplitude is proportional to the magnitude of $\bar{i}_h$ and its angular speed (in electrical radians per second) is $\omega_{hp} = \omega_h / h$, where ω_h is the angular speed of $\bar{i}_h$.

Neglecting the influence of the higher order harmonics for h>3, K_{wsh}=0 is of considerable importance. Hence, the MMF distribution given by (2) can be rewritten as follows:

$$F_s(\theta_s, t) = \frac{9N_s}{2\pi p} \Re_e\left(K_{ws1} \bar{i}_1(t) e^{jh\theta_s} + \frac{1}{3} K_{ws3} \bar{i}_3(t) e^{j3\theta_s} \right) \quad (3)$$

It can be seen from (3) that the MMF in the air gap produced by the nine stator phase windings has a non-sinusoidal spatial distribution, which depends exclusively on the instantaneous value of $\bar{i}_1$ and $\bar{i}_3$. The other stator current space vectors do not contribute to the air gap MMF and can be considered as degrees of freedom.

The electromagnetic torque is determined by:

$$T_e = \frac{\partial W_{co}}{\partial \theta_r} = \frac{9}{2} p \Re_e\left(\bar{\psi}_{mh} \times \bar{i}_h\right) \quad (4)$$

where $\bar{\psi}_{mh}$ is the kth space vector of flux linkage from permanent magnets.

It can be known from (3) and (4) that a constant torque can be obtained by operating the NP-FSPM motor in third harmonic current injection mode during normal operation. Hence, third harmonic currents can be injected in order to improve the flux distribution, power density and output torque, and the current controller of the drive system is required to track a set of non-sinusoidal current commands proportional to the given torque demand.

However, during loss of one phase, the NP-FSPM will operate as eight-phase asymmetrical machine. A large low-frequency pulsating torque appears, due to interaction between the fundamental current and the third harmonic EMF. The electromagnetic torque is expressed as (d-axis current component is set to 0):

$$\begin{aligned} T_{e1} &= \frac{9}{2} p \Re_e(\bar{\psi}_{mh} \times \bar{i}_1) \\ &= \frac{9p}{2}\left(\psi_{m1} i_{q1} + \frac{3}{2} \psi_{m3} i_{q1} (\cos 2\omega_1 t - \cos 4\omega_1 t) \right) \end{aligned} \quad (5)$$

Large $2\omega_1$ and $4\omega_1$ torque pulsations will appear when only the fundamental dq current reference is excited. Reconsidering the interaction between 3-order harmonic current and the fundamental EMF, the resulting torque can be obtained as:

$$\begin{aligned} T_{e3} &= \frac{9}{2} p \Re_e(\overline{\psi}_{mh} \times \bar{i}_3) \\ &= \frac{9p}{2}\left(\psi_{m3} i_{q3} + \frac{3}{2} \psi_{m1} i_{q3} (\cos 4\omega_1 t - \cos 2\omega_1 t) \right) \end{aligned} \tag{6}$$

It can be known from (6) that 3-order harmonic current will produce both second and fourth order torque harmonics. Finally, during fault-tolerant operation, the total electromagnetic torque can be calculated as:

$$T_e = T_{e1} + T_{e3} \tag{7}$$

To reduce the low-frequency torque harmonic to zero, a strict 3-order harmonic current should be injected. Hence, the third harmonic current to be injected is chosen as:

$$i_{q3} = \frac{-3\psi_{m3}}{\psi_{m1}} i_{q1} = \frac{E_3}{E_1} i_{q1} = k_3 i_{q1} \tag{8}$$

Therefore, optimal current phasors are found by setting the second-order and fourth-order torque harmonics to zero. It can be concluded that, during the loss of one phase, the restructured harmonic torque components T_{e3} can effectively offset the original harmonic torque components T_{e1}. Thus, in order to calculate the optimal set of excitation currents, prior information of the normalized back EMF induced in the stator phases is needed. The normalized back EMF information can be obtained from direct measurement of the back EMF at a given speed. Meanwhile, in order to get a high torque-to-volume ratio, the third harmonic current injection should be in accordance with expression (8). While in the non-fault operation, the other current space vectors are set to zero to reduce the stator copper losses.

III. Fault Tolerant Control

The fault-tolerant operation means that the drive system will continue to run in a satisfactory manner under fault conditions. As a first countermeasure after any fault detection, the corresponding inverter is forced to be electrically disconnected from the motor in order to eliminate its influence on the drive behavior. The fault detection technique is an important aspect in fault-tolerant operation, and several methods of fault diagnosis for motor drives have already been presented in the literature [14-15]. To achieve fault-tolerant operation of the proposed NP-FSPM, remedial strategies for open-circuit faults are proposed in this section. In the following analysis, a failure in one phase will be considered as an example. As emphasized in section II, employing a conventional sinusoidal phase current excitation, will inevitably result in an undesirable torque ripple in the unbalanced faulty operation. This problem can be overcome by adopting a third harmonic current injection compensative strategy which is aimed at effectively eliminating the low-frequency torque fluctuation.

A. Phase Current Reconstruction

According to amplitude invariant criterion and extended symmetrical component method, the nine-phase transformation from phase-variable model under stationary coordinate system to natural coordinate system for an arbitrary $0 \le \gamma < 2\pi$, can be deduced as:

$$\begin{bmatrix} i'_a \\ i'_b \\ \cdots \\ i'_i \end{bmatrix} = \begin{bmatrix} 1 & 0 & 1 & 0 & \cdots & 1 \\ \cos\gamma & \sin\gamma & \cos 3\gamma & \sin 3\gamma & \cdots & 1 \\ \cos 2\gamma & \sin 2\gamma & \cos 6\gamma & \sin 6\gamma & \cdots & 1 \\ \cos 3\gamma & \sin 3\gamma & \cos 9\gamma & \sin 9\gamma & \cdots & 1 \\ \cdots & \cdots & \cdots & \cdots & \cdots & \cdots \\ \cos 8\gamma & \sin 8\gamma & \cos 24\gamma & \sin 24\gamma & \cdots & 1 \end{bmatrix} \begin{bmatrix} \bar{i}_{1\alpha} \\ \bar{i}_{1\beta} \\ \bar{i}_{3\alpha} \\ \cdots \\ \bar{i}_{7\beta} \\ 0 \end{bmatrix} \tag{9}$$

where $\gamma = 2\pi/9$, i'_a, i'_b, ..., i'_i are the remaining phase currents under faulty condition, $\bar{i}_{1\alpha}$、$\bar{i}_{1\beta}$、$\bar{i}_{3\alpha}$...、$\bar{i}_{7\beta}$ are α-, β-axis components of stator currents in α_1-β_1, α_3-β_3, α_5-β_5 and α_7-β_7 plane respectively.

In normal condition, the 1st, 3rd, 5th, 7th harmonic currents produce 1st, 3rd, 5th, 7th harmonics of stator MMF respectively, and they are mapped into different orthogonal α-β planes respectively. The ninth equation denotes that the 9th harmonics of MMF is 0, and it also means that the sum of remaining phase currents is 0. When an open-circuit fault occurs in phase k_a, k_b, …, k_i, the corresponding current go down to zero and no common current return path is presented. From (9), it's clear that it contains nine equations and 8 unknowns after loss of phase "k_x", which means (9) has no solutions. It turns out that the current vectors are not independent any more.

It is worth noting that disturbance-free operation can be achieved if the harmonic distribution of the MMF, produced by the stator phase windings in the air gap, does not change in pre- and post-fault conditions. Since the reference space vector $\bar{i}_1$ and $\bar{i}_3$ are calculated by the control system to track the torque and flux set points, expression (9) cannot be satisfied if $\bar{i}_5$ and $\bar{i}_7$ are null simultaneously. Hence, neglecting the 5th or 7th harmonic, corresponding degrees of freedom can be used to minimize the copper loss. In order to produce smooth torque, the current vectors have to satisfy the following constraints:

$$i'_k = A i_s = 0 \tag{10}$$

where

$$A = \begin{bmatrix} \cos((k-1)\gamma) & \sin((k-1)\gamma) & \cos(3(k-1)\gamma) & \cdots & \sin(7(k-1)\gamma) \end{bmatrix}$$

$$i_s = \begin{bmatrix} \bar{i}_{1\alpha} & \bar{i}_{1\beta} & \bar{i}_{3\alpha} & \bar{i}_{3\beta} & \bar{i}_{5\alpha} & \bar{i}_{5\beta} & \bar{i}_{7\alpha} & \bar{i}_{7\beta} \end{bmatrix}^T .$$

From (10), it's clear that it contains one equation and four unknowns, the solution for fault-tolerant currents is not unique.

B. Optimization objective Analysis

There are many solutions for the stator phase currents satisfying above minimum torque ripple condition (8) and zero phase currents summation condition (10). But a unique solution for these conditions can be obtained by minimizing the stator copper loss. The instantaneous stator copper losses can be calculated as:

$$\begin{aligned} P_{cu} &= \frac{9}{2} R_s i_s^T i_s \\ &= \frac{9}{2} R_s (\bar{i}_{1\alpha}^2 + \bar{i}_{1\beta}^2 + \bar{i}_{3\alpha}^2 + \bar{i}_{3\beta}^2 + \bar{i}_{5\alpha}^2 + \bar{i}_{5\beta}^2 + \bar{i}_{7\alpha}^2 + \bar{i}_{7\beta}^2) \end{aligned} \tag{11}$$

Using Lagrangian multiplier λ for constrain (10), the objective function P for the system can be formed as:

$$P(\bar{i}_{1\alpha}, \bar{i}_{1\beta} \ldots, \bar{i}_{7\beta}, \lambda) = \frac{9}{2} R_s i_s^T i_s + \lambda A i \tag{12}$$

Zeroing the derivatives of the Lagrange function with respect to $\bar{i}_{5\alpha}$, $\bar{i}_{5\beta}$, $\bar{i}_{7\alpha}$, $\bar{i}_{7\beta}$ and λ leads to the following result:

$$\frac{\partial P}{\partial \bar{i}_{5\alpha}} = 0 \,,\ \frac{\partial P}{\partial \bar{i}_{5\beta}} = 0 \,,\ \ldots,\ \frac{\partial P}{\partial \lambda} = 0 \tag{13}$$

Therefore, the phase currents for the optimum operation of the machine under open circuit fault can be obtained as:

$$\begin{bmatrix} \bar{i}_{5\alpha} \\ \bar{i}_{5\beta} \end{bmatrix} = -\xi \left(\cos^2(5(k-1)\gamma) + \sin^2(5(k-1)\gamma) \right)^{-1} \cdot$$

$$\begin{bmatrix} \cos(5(k-1)\gamma)\cos((k-1)\gamma) & \cos(5(k-1)\gamma)\sin((k-1)\gamma) & \cos(5(k-1)\gamma)\cos(3(k-1)\gamma) & \cos(5(k-1)\gamma)\sin(3(k-1)\gamma) \\ \sin(5(k-1)\gamma)\cos((k-1)\gamma) & \sin(5(k-1)\gamma)\sin((k-1)\gamma) & \sin(5(k-1)\gamma)\cos(3(k-1)\gamma) & \sin(5(k-1)\gamma)\sin(3(k-1)\gamma) \end{bmatrix} \begin{bmatrix} \bar{i}_{1\alpha} \\ \bar{i}_{1\beta} \\ \bar{i}_{3\alpha} \\ \bar{i}_{3\beta} \end{bmatrix} \tag{14}$$

$$\begin{bmatrix} \bar{i}_{7\alpha} \\ \bar{i}_{7\beta} \end{bmatrix} = -\xi \left(\cos^2(7(k-1)\gamma) + \sin^2(7(k-1)\gamma) \right)^{-1} \cdot$$

$$\begin{bmatrix} \cos(7(k-1)\gamma)\cos((k-1)\gamma) & \cos(7(k-1)\gamma)\sin((k-1)\gamma) & \cos(7(k-1)\gamma)\cos(3(k-1)\gamma) & \cos(7(k-1)\gamma)\sin(3(k-1)\gamma) \\ \sin(7(k-1)\gamma)\cos((k-1)\gamma) & \sin(7(k-1)\gamma)\sin((k-1)\gamma) & \sin(7(k-1)\gamma)\cos(3(k-1)\gamma) & \sin(7(k-1)\gamma)\sin(3(k-1)\gamma) \end{bmatrix} \begin{bmatrix} \bar{i}_{1\alpha} \\ \bar{i}_{1\beta} \\ \bar{i}_{3\alpha} \\ \bar{i}_{3\beta} \end{bmatrix} \tag{15}$$

where ξ is a faulty condition quantity and its value is 1 or 0, corresponding to faulty or healthy mode, respectively.

The remaining phase currents can be easily solved in eq. (9). This group of currents can produce minimized stator copper loss when the 1st, 3rd harmonics of stator MMF are kept unchanged after phase "k_x" is open-circuit.

IV. Simulation Results

A. Control Method

Since the traditional rotor-flux-oriented control strategy cannot be applied to the NP-FSPM motor directly, a stator-flux-oriented (SFO) *dq* equation of the motor in the rotor reference frame is developed [16]. It can be found that the rotor position of the maximum PM flux linkage is defined as the d-axis, while the *q*-axis advances the *d*-axis by 90°electrical degrees (equivalent to 2.64° in mechanical degree). The development of the *dq*-axes is crucial for the development of this SFO fault-tolerant control strategy. It has been known that the *q*- and *d*-axis components of armature currents correspond to the production of torque and flux, respectively. When the *d*-axis component of armature current is maintained, the stator-PM flux-linkage will be constant. Thus, by setting the *q*-axis component of armature current invariant before and after the fault, the electromagnetic torque of the NP-FSPM motor can be maintained.

Fig. 3 shows the control block diagram of the NP-FSPM motor drive, in which the SFO fault-tolerant control is incorporated. By employing a proportional-integral (PI) regulator, the difference between the reference speed and the actual speed determines the reference electromagnetic torque, which is directly proportional to the *q*-axis component of armature current. The space vector pulse width modulation (SVPWM) controller is employed to drive the inverter. The controller can use ξ to control the scheme selection and activation. Switching to healthy operation mode, the reference value of the first current space vector $\bar{i}_1$ is calculated by the control system in order to satisfy the demand of torque and flux, and the third harmonic current injection rate was obtained by (8) to enhance the output torque, whereas the remaining current space vectors are usually set to zero. As to the fault tolerant implementation, the harmonic components in the current references are generated by the control system itself, which were calculated by (14) and (15).

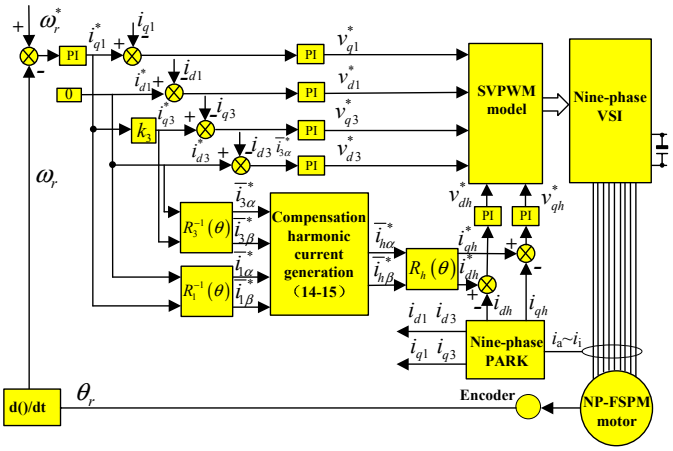

Fig. 3 Fault-tolerant control scheme block diagram for the NP-FSPM motor drive.

It should be noted that the fault-tolerant harmonic currents are performed in the $\alpha\beta$ reference frame. Hence, the dq currents have to be deduced from $\alpha\beta$ currents by a proper transformation, which can be expressed as:

$$R_h(\theta)=\begin{bmatrix}\cos h\theta & \sin h\theta\\ -\sin h\theta & \cos h\theta\end{bmatrix} \tag{16}$$

where θ is electrical degree.

B. Simulation Results

To evaluate the proposed remedial control strategy, a transient Matlab/Simulink simulation model of the NP-FSPM motor drive is developed as shown in Fig. 4. All the simulation parameters used in these studies have remained the same, which are shown in Table I.

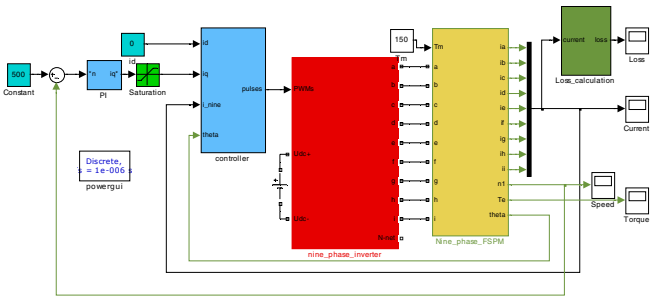

Fig. 4 Simulink model of NP-FSPM drive system.

Table I
MOTOR PARAMETERS

Rated output power	10 kW
Rated current (rms)	4.83 A
Rated frequency	283 Hz
Rated speed	500 rpm
No. of pole-pairs in rotor	34
No. of pole-pairs in stator	36
Resistance per coil	1.3
D-axis inductance	80 mH
Q-axis inductance	72 mH
D-axis magnetic flux	0.224 Wb
Rotary inertia	0.05 kg.m^2

For the purpose of quantitative evaluation of torque performance of the FSPM motor drive under normal and fault-tolerant operations, a torque ripple factor is defined as:

$$K_T=(T_{\max}-T_{\min})/T_{av}\times 100\% \tag{17}$$

where $T_{\max}$, $T_{\min}$ and T_{av} are the maximum, minimum, and average values of the output torque, respectively.

On this simulation, the NP-FSPM drive system was fed by nine-phase voltage source inverter (VSI) using basic SFO-dq strategy and the controller is required to track a set of non-sinusoidal current commands to produce the rated torque of 150 (Nm) at a rotor speed of 500rpm. The stator excitation currents (analogous to q-axis current space vector in Fig. 5) under normal condition during 0.01~0.02s are shown in Fig. 6 (b). The normal currents constitute only the fundamental and third-harmonic components, which are proportional to the frequency components of the back EMFs of the machine.

A sudden winding open-circuit fault was emulated and applied in phase A at t=0.02s, then ξ is set to be 1 at t=0.03s. Fig. 5 shows the dq stator currents during pre- and post open-circuit fault condition, the 1st, 3rd harmonics of stator currents are kept unchanged after phase A is open circuit, and the 5th, 7th harmonic currents are used to produce smooth torque. Fig. 6 (c) and (d) shows the stator excitation currents in the fault operation and fault-tolerant operation, respectively.

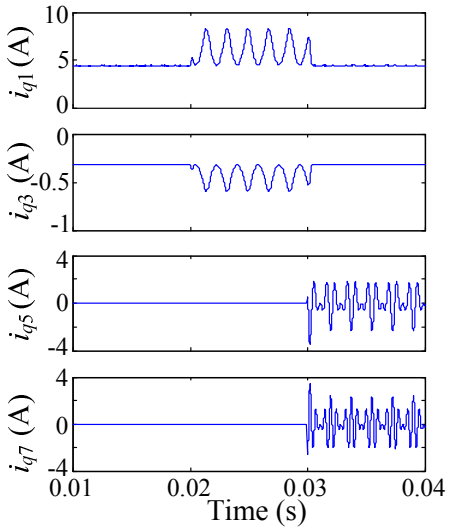

Fig. 5 Stator q-axis currents.

Fig. 7 shows the speed and torque waveforms. As will be seen, due to the back EMF harmonics and fault condition, a torque ripple of 13.3% exists under such open-circuit fault conditions. Pulsation with double fundamental frequency is observed in both the speed and torque. The pulsation is caused by the 3rd harmonic of stator MMF. Then, the proposed fault-tolerant control strategy is evaluated at t=0.03s. It can be observed that the motor drive can online switch to the fault-tolerant mode. The torque oscillations are reduced efficiently by the proposed method, and the system can operate continuously and steadily after the open-circuit fault occurrence.

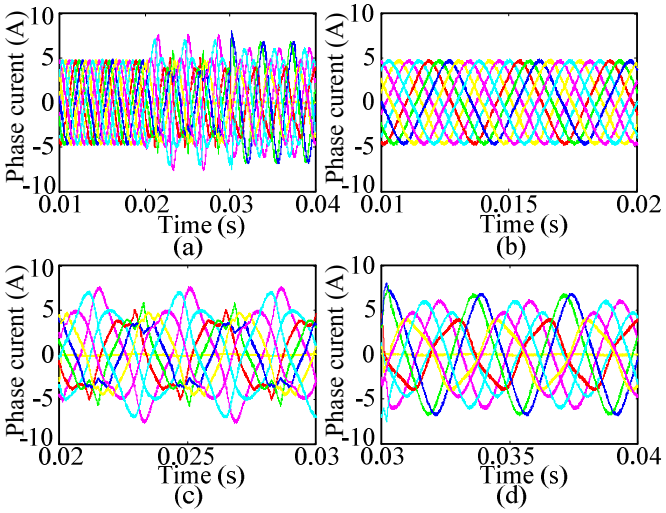

Fig. 6 Stator excitation currents. (a) Mode switching operation. (b) Normal operation. (c) Fault operation. (d) Fault-tolerant operation.

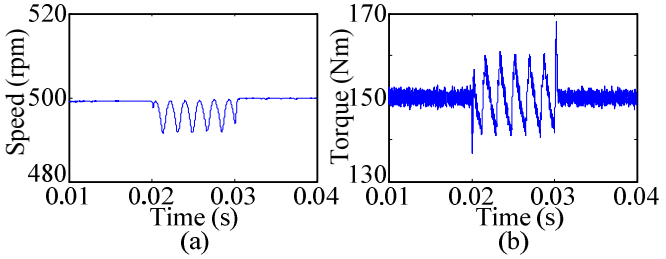

Fig. 7 Dynamic simulation results of fault-tolerant operation. (a) Speed waveform. (b) Torque waveform.

By using the proposed remedial strategy, the locus of the $\alpha\beta$ stator currents has been observed in Fig. 8, verifying that the 5-order and 7-order harmonic currents injected in the stator windings are used to produce circular rotating fundamental and 3-order harmonic MMFs during fault-tolerant operation.

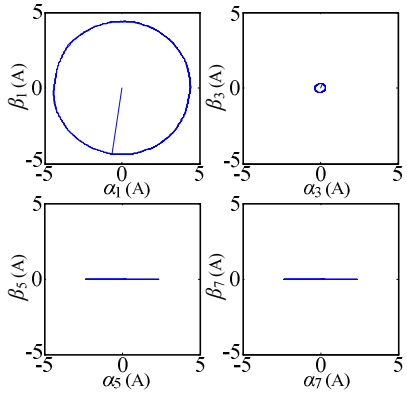

Fig. 8 Locus of fault-tolerant currents.

V. Conclusion

This paper calculates the average torque and the pulsating torque components of the NP-FSPM motor in steady-state. The new nine-phase decoupled transformation matrix under open-phase fault is built, and then the fault-tolerant control method is proposed based on the multiple space vector representation of nine-phase quantities, and it can be used for up to more open stator phases by applying a convenient rotating reference frame with $\alpha\beta$ components. Finally, simulations for one phase open fault have been carried out. The results indicate that the proposed tolerant control method in this paper can reduce the low-frequency torque oscillations under open-phase fault significantly, which ensures that the motor continues to operate steadily.

References

[1] M. Cheng, W. Hua, J. Zhang, and W. Zhao, "Overview of stator-permanent magnet brushless machines," *IEEE Trans. Ind. Electron.*, vol. 58, no. 11, pp. 5087-5101, Nov., 2011.

[2] J. T. Chen, Z. Q. Zhu, S. Iwasaki, and R. P. Deodhar, "A novel hybrid-excited switched-flux brushless AC machine for EV/HEV applications," *IEEE Trans. Vehicular Technology*, vol. 60, no. 4, pp. 1365-1373, May 2011.

[3] R. Cao, C. Mi, M. Cheng, "Quantitative comparison of flux-switching permanent magnet motors with interior permanent magnet motor for EV, HEV, and PHEV applications,". *IEEE Trans. Magn.*, vol. 48, no. 8, pp. 2374-2384, Aug. 2012.

[4] M. Cheng, C. C. Chan, "General requirement of traction motor drives," in D. Crolla, D.E. Foster, T. Kobayashi and N. Vaughan (Eds.) *Encyclopedia of Automotive Engineering*, John Wiley & Sons, Ltd: Chichester. DOI: 10.1002/9781118354179.auto041, 2014.

[5] K. T. Chau, C. C. Chan, and C. Liu, "Overview of permanent-magnet brushless drives for electric and hybrid electric vehicles," *IEEE Trans. Industrial Electronics*, vol. *55,* no. *6,* pp. *2246-2257,* Jun. 2008.

[6] T. Morizane and E. Masada, "Study on the feasibility of application of linear induction motor for vertical movement," *IEEE Trans. Magn.*, vol. 29, no. 6, pp. 2938-2940, 1993.

[7] B. A. Welchko, T. A. Lipo, T. M. Jahns, S. E. Schulz, "Fault tolerant three-phase AC motor drive topologies: a comparison of features, cost, and limitations," *IEEE Trans. Power Electron.*, vol. 19, no. 4, pp. 1108-1116, July 2004.

[8] M. A. Shamsi-Nejad, B. Nahid-Mobarakeh, S. Pierfederici, and F. Meibody-Tabar, "Fault tolerant and minimum loss control of double-star synchronous machines under open phase conditions," *IEEE Trans. Ind. Electron.*, vol. 55, no. 5, pp. 1956-1965, May 2008.

[9] W. Zhao, M. Cheng, W. Hua, H. Jia, "Back-EMF harmonic analysis and fault-tolerant control of flux-switching permanent-magnet machine with redundancy," *IEEE Trans. Ind. Electron.*, vol. 58, no. 5, pp. 1926-1935, May 2011.

[10] Toliyat H A, "Analysis and simulation of five phase variable speed induction motor drives under asymmetrical connections," *IEEE Trans. Power Electron.*. vol. 13, no. 4, pp. 748-756, July 1998.

[11] N. Bianchi, S. Bolognani, M. D. Pre, "Strategies for the fault-tolerant current control of a five-phase permanent- magnet motor," *IEEE Trans. Ind. Appl.*, vol. 43, no. 4, pp. 960-970, July 2007.

[12] Suman D, Leila P, "An optimal control technique for multiphase PM machines under open-circuit faults," *IEEE Trans. Ind. Electron.*, vol. 55, no. 5, pp. 1988-1995, May 2008.

[13] G. Grandi, G, Serra, A. Tani, "General analysis of multiphase systems based on space vector approach," in *Pro. Int. Conf. EPE-PEMC*, Portoroz, Slovenia, 2006, pp. 834-840.

[14] S. M. Jung, J. S. Park, H. W. Kim, K. Y. Cho, and M. J. Youn, "An MARS-based diagnosis of open-circuit fault in PWM voltage-source inverters for PM synchronous motor drive systems," *IEEE Trans. Power Electron.*, vol. 28, no. 5, pp. 2514-2526, May 2013.

[15] J. Urresty, J. R. Riba, M. Delgado, and L. Romeral, "Detection of demagnetization faults in surface-mounted permanent magnet synchronous motors by means of the zero-sequence voltage component," *IEEE Trans. Energy Convers.*, vol. 27, no. 1, pp. 42-51, Mar. 2012.

[16] W. Zhao, M. Cheng, K. T. Chau, Wei Hua, "Stator-flux-oriented fault-tolerant control of flux-switching permanent-magnet motors," *IEEE Trans. Magn.*, vol. 47, no. 10, pp. 4191-4194, Oct. 2011.